Substrate Channeling Hot Paper

Deutsche Ausgabe: DOI: 10.1002/ange.201603183
Internationale Ausgabe: DOI: 10.1002/anie.201603183

Directional Regulation of Enzyme Pathways through the Control of Substrate Channeling on a DNA Origami Scaffold

Guoliang Ke, Minghui Liu, Shuoxing Jiang, Xiaodong Qi, Yuhe Renee Yang, Shaun Wootten, Fei Zhang, Zhi Zhu, Yan Liu, Chaoyong James Yang,* and Hao Yan**

Abstract: *Artificial multi-enzyme systems with precise and dynamic control over the enzyme pathway activity are of great significance in bionanotechnology and synthetic biology. Herein, we exploit a spatially addressable DNA nanoplatform for the directional regulation of two enzyme pathways (G6pDH–MDH and G6pDH–LDH) through the control of NAD^+ substrate channeling by specifically shifting NAD^+ between the two enzyme pairs. We believe that this concept will be useful for the design of regulatory biological circuits for synthetic biology and biomedicine.*

The metabolism of living systems involves myriads of delicate multi-enzyme systems and the precise and dynamic control of enzymes and substrates.[1] Therefore, artificial multi-enzyme systems are of interest in various areas, such as synthetic biology, biocatalysis, nanofabrication, and biomedicine. Particularly, the construction of a smart stimuli-triggered multi-enzyme system that directionally activates different enzyme pathways in response to different environmental conditions (e.g., different stimulants, different substrate levels) is critical for their application, for example, in enzyme regulatory circuitry and signal-transduction pathways.[2] Structural DNA nanotechnology[3] has been a powerful platform for the design of artificial multi-enzyme reaction pathways,[4] with the advantages of programmable assembly, nanometer positional precision, and dynamic structural control. Recently, the activity of a single enzyme pathway (i.e., GOx/HRP) was successfully controlled by changing the inter-enzyme distance on a DNA scaffold; however, this system suffers from relatively slow and inefficient regulation as it is based on the mechanical control of large molecules such as enzymes.[5] Alternatively, a strategy that is based on the spatial control of small molecules such as substrates is expected to be faster, easier, and more efficient for the directional regulation of multiplex enzyme pathways in a multi-enzyme network in response to different stimulants, and its development is thus highly desirable.

Many natural cascade enzyme pathways rely on substrate channeling, which passes the intermediary metabolic product of one enzyme directly to another enzyme without its release into solution, to expedite the reaction flow as well as to prevent the intermediates from being consumed by competing reactions.[6] Inspired by this mechanism, we recently used NAD^+-modified single-stranded DNA (ssDNA) to realize an artificial swinging arm for substrate channeling between two dehydrogenase enzymes on a linear one-dimensional DNA scaffold.[7] The swinging arm could significantly increase the activity of the two enzymes assembled together. Considering this important role of substrate channeling, we hypothesized that the mechanical control of the substrate channeling position could be a new approach for regulating the activity of cascaded enzymes. Meanwhile, a two-dimensional DNA scaffold will enable the construction of a more complex enzyme network with more enzyme pathways, as well as more directions of substrate channeling, thus enabling the directional regulation of substrate channeling for controlling the activities of enzymatic pathways. Herein, we demonstrate for the first time that the directional control of substrate channeling is an efficient approach for the directional regulation of multi-enzyme reaction pathways on a DNA origami scaffold.

As shown in Figure 1a, we constructed a model multi-enzyme system arranged on a rectangular DNA origami platform that involves three dehydrogenases (glucose-6-phosphate dehydrogenase (G6pDH), malate dehydrogenase (MDH), and lactate dehydrogenase (LDH)) and a cofactor (nicotinamide adenine dinucleotide (NAD^+)). G6pDH uses NAD^+ to oxidize glucose-6-phosphate, and the NAD^+ is turned into NADH, which can be used by both MDH and LDH as the reducing agent to reduce oxaloacetate to malate and pyruvate to lactate, respectively. The NAD^+ substrate channeling has a great influence on the activities of the two-enzyme cascade system (G6pDH–MDH or G6pDH–LDH): the two-enzyme cascade system is expected to achieve high activity when the co-substrate is tethered between the two enzymes and allowed to swing between them; a lower activity is expected when the co-substrate is far away from both enzymes. Thus by switching the position of the NAD^+ substrate channeling, the relative activities of the two two-enzyme pathways (G6pDH–MDH and G6pDH–LDH) can be regulated. As shown in Figure 1a, when NAD^+ is tethered to

[*] G. Ke, Dr. M. Liu, S. Jiang, Dr. X. Qi, Y. R. Yang, S. Wootten, Dr. F. Zhang, Prof. Y. Liu, Prof. H. Yan
Center for Molecular Design and Biomimetics, Biodesign Institute and School of Molecular Sciences at Arizona State University
Tempe, Arizona 85287 (USA)
E-mail: hao.yan@asu.edu
yan_liu@asu.edu
G. Ke, Prof. Z. Zhu, Prof. C. J. Yang
The MOE Key Laboratory of Spectrochemical Analysis and Instrumentation
State Key Laboratory of Physical Chemistry of Solid Surfaces
Collaborative Innovation Center of Chemistry for Energy Materials
Department of Chemical Biology
College of Chemistry and Chemical Engineering
Xiamen University, Xiamen, 361005 (China)
E-mail: cyyang@xmu.edu.cn
Supporting information and the ORCID identification number(s) for the author(s) of this article can be found under http://dx.doi.org/10.1002/anie.201603183.

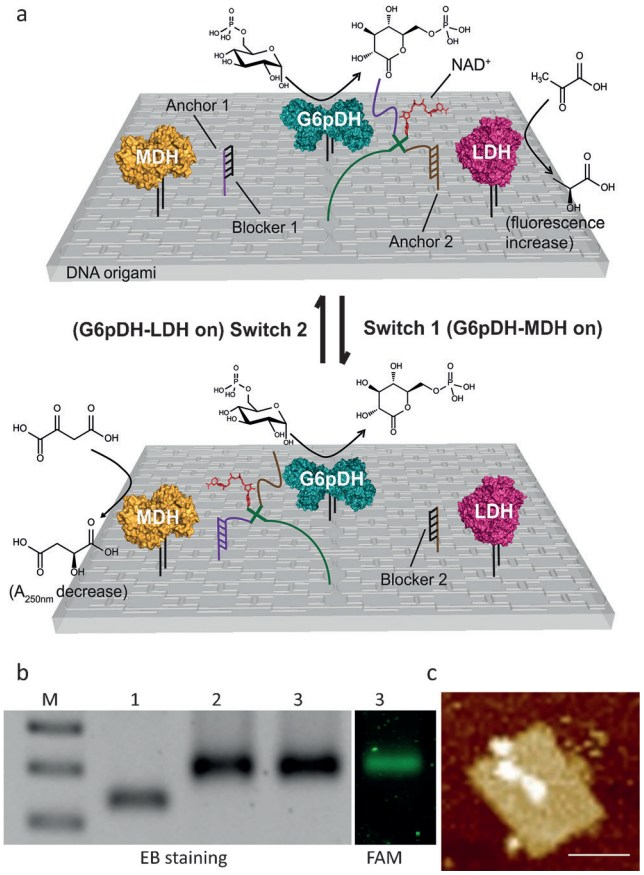

Figure 1. Design and characterization of the enzyme pathway regulation system on DNA origami. a) The nanostructured complex consisting of G6pDH, MDH, LDH, and NAD^+-anchored HJ on a rectangular DNA origami platform. In the presence of switch 1, the NAD^+ substrate channeling binds to anchor 1 and is located between G6pDH and MDH, thus activating the G6pDH–MDH pathway. In the presence of switch 2, the substrate channeling is located between G6pDH and LDH, activating the G6pDH–LDH pathway. b) Characterization of the assembled DNA origami complex with 1.2% agarose gel (left: EB staining for DNA detection; right: fluorescence imaging for FAM detection). Lane 1: rectangular origami; lane 2: rectangular origami with G6pDH/MDH/LDH; lane 3: rectangular origami with G6pDH/MDH/LDH and FAM-labeled HJ. c) AFM image of the rectangular origami with G6pDH/MDH/LDH and HJ. Scale bar: 50 nm.

anchor 1 for substrate channeling between G6pDH and MDH, the G6pDH–MDH and G6pDH–LDH pathways are activated and deactivated, respectively. The opposite activation pattern is observed when the substrate channeling is switched to anchor 2, which is located between G6pDH and LDH. This positional switching of substrate channeling is made possible by dynamic DNA toehold-mediated strand displacement.[8] The cofactor NAD^+ was attached to the end of one arm of a four-arm Holliday junction (HJ; see the Supporting Information, Figure S8 and Table S2), which is linked to the DNA origami through an opposite arm at a position with appropriate distances to the three enzymes. The other two HJ arms have single-stranded extensions that allow for the positional switching of the cofactor by selectively binding with one of the two anchors located between the enzyme pairs.

The protein–DNA conjugates were synthesized by using a bifunctional succinimidyl 3-(2-pyridyldithio)propionate (SPDP) linker[7,9] (for LDH) or a HaloTag[10] genetically engineered on the protein (for MDH and G6pDH; Figure S1–S4). Through sequence-specific hybridization of the DNA tags linked to the enzymes with the extended anchoring probes on the origami, all three enzymes were successfully attached to a rectangular DNA origami (ca. $60 \times 90\ nm^2$). The assembly yield of all three enzymes on the DNA origami was estimated to be higher than 80%, based on an agarose gel mobility shift assay (Figure 1b and Figure S7). Atomic force microscopy (AFM) images (Figure 1c and Figure S7) showed that the locations of the proteins matched their expected positions on the DNA origami (see Figure S19 for details). To confirm the attachment of the four-arm HJ on the DNA origami, we labeled the HJ with an organic fluorescent dye (FAM) in place of the cofactor (Figure S8b) and subjected the constructed assembly to native gel electrophoresis (Figure 1b, lane 3). From the overlay of the EB staining and the fluorescence gel imaging, the dye stayed in the same band as the protein–origami assembly, indicating the successful attachment of the HJ on the DNA origami together with all three enzymes.

In a proof-of-concept experiment to demonstrate the positional switching of the HJ between the two anchoring sites on the DNA origami, we utilized fluorescence spectroscopy for the real-time monitoring of the switching process. As shown in Figure 2a, green (AF488) and red (TAMRA) fluorescent dyes were used to label the two anchors on the origami scaffold, respectively. On the HJ, a quencher (BHQ1) was attached to both arms that will bind with the anchors (Figure S8c, Table S2). In the presence of switch 1 (ACE, see Table S3 and Figure S9–12 for the optimization of the switch length), blocker 1 (E*C*A*) is removed to unlock anchor 1 (AC), enabling HJ to bind with anchor 1 (via AA* pairing, status II), which brings the quencher near the green dye and decreases the green emission (Figure 2b). The addition of the block strand (E*C*A*) releases the HJ from anchor 1 back to the middle position (status I), and the green fluorescence is recovered. Similarly, upon addition of switch 2 (BDF) and blocker 2 (F*D*B*), the position of the HJ can be changed between anchor 2 (BD via BB* pairing, status III) and the middle position (status I), resulting in the quenching and recovery of the red emission of TAMRA, respectively (Figure 2c). These results also show that the switching between the binding states was relatively fast (within a few minutes, shown in Figure 2b,c) and reversible (Figure 2d).

The activity modulation of each enzyme pathway was then achieved through optimization of the spacer length and the distance between the enzymes. In these experiments, NAD^+ was anchored on the free arm of the HJ (Figure S8d, Table S2) through a disuccinimidyl suberate (DSS) linking strategy[7,9] (Figures S5 and S6). G6pDH and the respective secondary enzyme (MDH or LDH) were attached to the origami scaffold, and the anchor strands 1 and 2 were located between the respective enzyme pairs. Taking G6pDH–MDH as an example (Figure 3a), this enzyme pathway was activated when the HJ binds to anchor 1, which brings the NAD^+ substrate channeling closer to MDH; however, this enzyme pathway is blocked when the HJ binds to anchor 2 so that the substrate channeling is kept further away from MDH. The

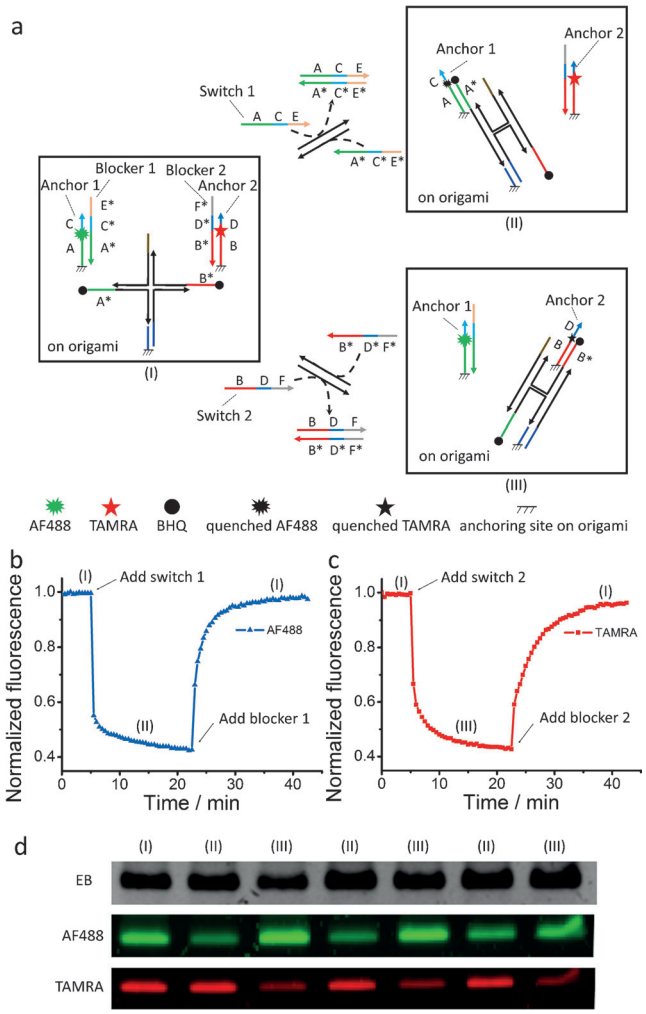

Figure 2. Fluorescence study of the positional switching of HJ binding. a) The toehold-mediated strand displacement strategy for controlling the HJ binding position on the DNA origami. b) Real-time AF488 fluorescence study of HJ binding to the left anchor and returning to the middle position. c) Real-time TAMRA fluorescence study of HJ binding to the right anchor and returning to the middle position. d) Fluorescence agarose gel characterization of the reversible binding of HJ at different sites for several cycles.

normalized activity ratio of the pathway in the active and inactive states was used as the criterion for the optimization of the design parameters (see Figures S13–S17 and Table S4 for the normalization method).

The first parameter to be optimized was the length of the single-stranded polythymidine (T) linker between NAD^+ and HJ at a fixed inter-enzyme distance of approximately 20 nm. Poly(T) spacers with different lengths (T0, T5, T10, T15, and T20) were utilized for both pathways. The results (Figure 3b) showed that the activity ratio of G6pDH–MDH increased as the poly(T) spacer was shortened, largely owing to the decreased activity of the inactive state, probably because the NAD^+ with a shorter spacer was further away from the secondary enzyme (MDH) when it was anchored in the inactive state. For the G6pDH–LDH pathway (Figure 3e), the activity ratio of the active and inactive states showed a maximum value at T5, and decreased as the spacer length increased. As the spacer length should be the same for both

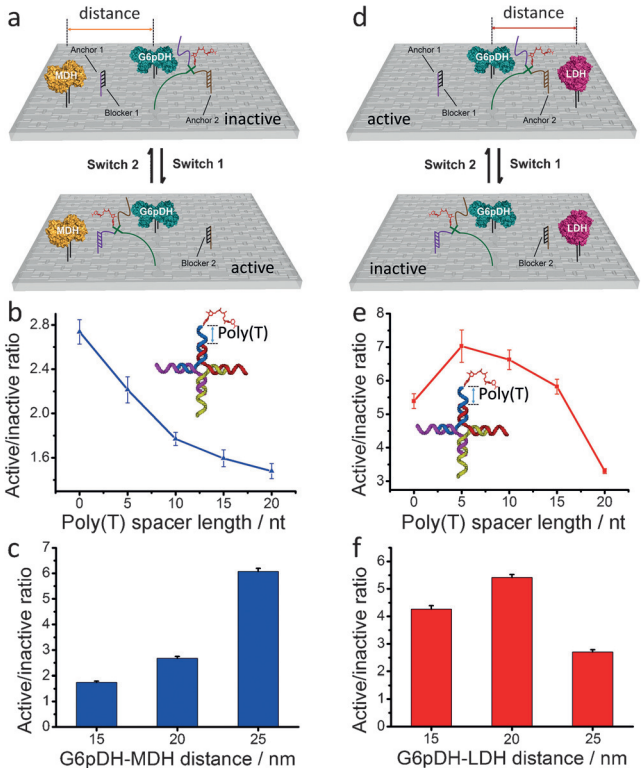

Figure 3. Optimization of the activity regulation of G6pDH–MDH (a–c) and G6pDH-LDH (d–f) by changing the substrate channeling position. The poly(T) spacer length between NAD^+ and HJ (b, e) and the inter-enzyme distance (c, f) were optimized. The normalized activity ratio of the pathway in the active and inactive states was used as the criterion for optimization.

pathways, we chose to use T0 as the spacer (i.e., no spacer between NAD^+ and the HJ), a condition for which both pathways reliably achieved high on/off activity ratios. Furthermore, by fixing the position of G6pDH, we also changed the position of MDH (or LDH) to control the enzyme distance (Figure 3c and Figure 3f) using the optimized NAD^+ spacer length. The activity assay results show that the best distances for G6pDH–MDH and G6pDH–LDH were 25 and 20 nm, respectively, which were used for all further enzyme pathway regulation experiments. The difference is mostly due to the inherent properties of MDH and LDH (e.g., in terms of size and shape).[2,7] These results clearly confirm that we can successfully regulate each enzyme pathway by changing the position of their substrate channeling.

Finally, we achieved the directional regulation of the enzyme pathways by using short ssDNA to alternatively control the on and off switching of the G6pDH–MDH and G6pDH–LDH pathways on the DNA scaffold. As shown in Figure 4a,b, in the presence of switch 1, the HJ binds to anchor 1 to achieve substrate channeling between G6pDH and MDH, thus activating the G6pDH–MDH pathway (its activity can be monitored by a significant absorption decrease at 250 nm in Figure 4a).Simultaneously, the G6pDH–LDH pathway was blocked (indicated by the small increase in the fluorescence intensity at 590 nm in Figure 4b). Conversely, in the presence of switch 2, HJ binds to anchor 2 and brings the substrate channeling close to LDH, turning on the G6pDH–

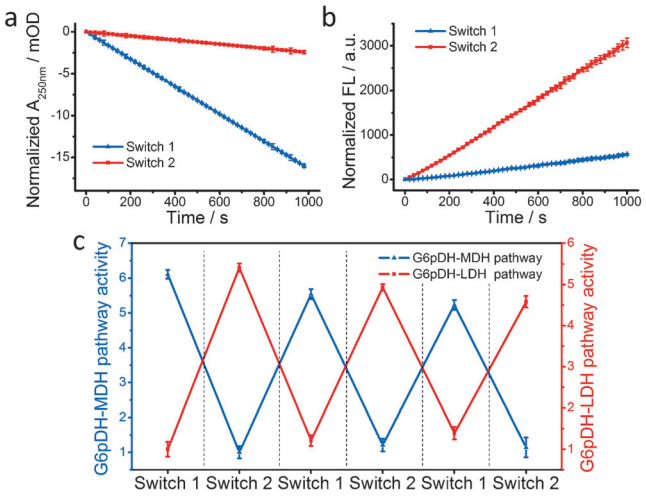

Figure 4. Directional regulation of enzyme pathways by DNA switches. a) G6pDH–MDH pathway activity in the presence of switch 1 or 2. b) G6pDH–LDH pathway activity in the presence of switch 1 or 2. c) Regulatory cycling of the enzyme pathway activity. All enzyme activities were normalized to the respective activity in the initial status. A twofold amount of switch 1 or 2 was added for each conformational change.

LDH pathway (indicated by a strong increase in the fluorescence intensity) and shutting down the G6pDH–MDH pathway (indicated by the small absorption decrease at 250 nm). The optimized on/off activity ratio for both pathways is approximately five- to sevenfold. As shown in Figure 4c, the reversibility of the enzyme pathway regulation was also successfully confirmed by several cycles of activity regulation.

In conclusion, we have demonstrated the directional regulation of enzyme pathways in an artificial multi-enzyme network by controlling the position of the substrate channeling. The artificial enzyme network exhibited different activities for the two enzyme pathways in response to different external stimuli (different regulatory DNA single strands) with fast response and good reversibility: Switch 1 activated the G6pDH–MDH pathway and shut down the G6pDH–LDH pathway whereas switch 2 activated the G6pDH–LDH pathway and reduced the G6pDH–MDH pathway. To the best of our knowledge, this is the first study that demonstrates the directional regulation of multiple enzyme pathways through the control of substrate channeling on functional DNA scaffolds. In the future, this strategy for the activity regulation of enzyme pathways through the control of substrate channeling should be applicable to the design of smart enzyme networks involved in feedback or feed-forward control and synergistic or antagonistic effects,[11] as well as the development of functional catalytic devices for energy and material converters and regulatory biological circuits for synthetic biology and biomedicine.[12]

Acknowledgements

We are grateful for a DOD-Navy-ONR MURI award (W911NF-12-1-0420) and an Army Research Office grant (W911NF-11-1-0137) and thank the National Science Foundation (14030615), the National Science Foundation of China (21325522, 21422506, 21275122, 21521004), the Program for Changjiang Scholars and Innovative Research Team in University (IRT13036), and the China Scholarship Council Fellowship for financial support.

Keywords: DNA origami · enzymes · NADH · self-assembly · substrate channeling

How to cite: *Angew. Chem. Int. Ed.* **2016**, *55*, 7483–7486
Angew. Chem. **2016**, *128*, 7609–7612

[1] D. F. Savage, B. Afonso, A. H. Chen, P. A. Silver, *Science* **2010**, *327*, 1258–1261.
[2] J. L. Fu, M. H. Liu, Y. Liu, H. Yan, *Acc. Chem. Res.* **2012**, *45*, 1215–1226.
[3] a) N. C. Seeman, *J. Theor. Biol.* **1982**, *99*, 237–247; b) P. W. K. Rothemund, *Nature* **2006**, *440*, 297–302; c) P. Yin, H. M. T. Choi, C. R. Calvert, N. A. Pierce, *Nature* **2008**, *451*, 318–322; d) E. S. Andersen, M. Dong, M. M. Nielsen, K. Jahn, R. Subramani, W. Mamdouh, M. M. Golas, B. Sander, H. Stark, C. L. P. Oliveira, J. S. Pedersen, V. Birkedal, F. Besenbacher, K. V. Gothelf, J. Kjems, *Nature* **2009**, *459*, 73–76; e) T. Liedl, B. Högberg, J. Tytell, D. E. Ingber, W. M. Shih, *Nat. Nanotechnol.* **2010**, *5*, 520–524; f) A. Rajendran, M. Endo, H. Sugiyama, *Angew. Chem. Int. Ed.* **2012**, *51*, 874–890; *Angew. Chem.* **2012**, *124*, 898–915; g) B. Saccà, C. M. Niemeyer, *Angew. Chem. Int. Ed.* **2012**, *51*, 58–66; *Angew. Chem.* **2012**, *124*, 60–69; h) F. Zhang, J. Nangreave, Y. Liu, H. Yan, *J. Am. Chem. Soc.* **2014**, *136*, 11198–11211; i) T. Gerling, K. F. Wagenbauer, A. M. Neuner, H. Dietz, *Science* **2015**, *347*, 1446–1452; j) X. Li, C. Zhang, C. H. Hao, C. Tian, G. S. Wang, C. D. Mao, *ACS Nano* **2012**, *6*, 5138–5142.
[4] a) C. M. Niemeyer, J. Koehler, C. Wuerdemann, *ChemBioChem* **2002**, *3*, 242–245; b) O. I. Wilner, Y. Weizmann, R. Gill, O. Lioubashevski, R. Freeman, I. Willner, *Nat. Nanotechnol.* **2009**, *4*, 249–254; c) M. Erkelenz, C. H. Kuo, C. M. Niemeyer, *J. Am. Chem. Soc.* **2011**, *133*, 16111–16118; d) Y. M. Fu, D. D. Zeng, J. Chao, Y. Q. Jin, Z. Zhang, H. J. Liu, D. Li, H. W. Ma, Q. Huang, K. V. Gothelf, C. H. Fan, *J. Am. Chem. Soc.* **2013**, *135*, 696–702.
[5] a) L. Xin, C. Zhou, Z. Q. Yang, D. S. Liu, *Small* **2013**, *9*, 3088–3091; b) Y. W. Hu, F. Wang, C. H. Lu, J. Girsh, E. Golub, I. Willner, *Chem. Eur. J.* **2014**, *20*, 16203–16209; c) J. L. Fu, M. H. Liu, Y. Liu, N. W. Woodbury, H. Yan, *J. Am. Chem. Soc.* **2012**, *134*, 5516–5519.
[6] E. W. Miles, S. Rhee, D. R. Davies, *J. Biol. Chem.* **1999**, *274*, 12193–12196.
[7] J. L. Fu, Y. R. Yang, A. Johnson-Buck, M. H. Liu, Y. Liu, N. G. Walter, N. W. Woodbury, H. Yan, *Nat. Nanotechnol.* **2014**, *9*, 531–536.
[8] D. Y. Zhang, G. Seelig, *Nat. Chem.* **2011**, *3*, 103–113.
[9] a) M. H. Liu, J. L. Fu, C. Hejesen, Y. H. Yang, N. W. Woodbury, K. Gothelf, Y. Liu, H. Yan, *Nat. Commun.* **2013**, *4*, 2127; b) Z. Zhao, J. L. Fu, S. Dhakal, A. Johnson-Buck, M. H. Liu, T. Zhang, N. W. Woodbury, Y. Liu, N. G. Walter, H. Yan, *Nat. Commun.* **2016**, *7*, 10619.
[10] a) G. V. Los, K. Wood, *Methods Mol. Biol.* **2007**, *356*, 195–208; b) C. Timm, C. M. Niemeyer, *Angew. Chem. Int. Ed.* **2015**, *54*, 6745–6750; *Angew. Chem.* **2015**, *127*, 6849–6854.
[11] J. S. Hubbard, E. R. Stadtman, *J. Bacteriol.* **1967**, *93*, 1045–1055.
[12] a) H. Liang, X. B. Zhang, Y. Lv, L. Gong, R. Wang, X. Zhu, R. Yang, W. Tan, *Acc. Chem. Res.* **2014**, *47*, 1891–1901; b) N. Chen, J. Li, H. Y. Song, J. Chao, Q. Huang, C. H. Fan, *Acc. Chem. Res.* **2014**, *47*, 1720–1730; c) Y. R. Yang, Y. Liu, H. Yan, *Bioconjugate Chem.* **2015**, *26*, 1381–1395.

Received: March 31, 2016
Published online: May 9, 2016